

Understanding the Performance Horizon of the Latest ML Workloads with NonGEMM Workloads

Rachid Karami

Electrical Engineering and Computer Science
University of California, Irvine
Irvine, USA
karamir@uci.edu

Sheng-Chun Kao

Mountain View, USA
chuchu40507@gmail.com

Hyoukjun Kwon

Electrical Engineering and Computer Science
University of California, Irvine
Irvine, USA
hyoukjun.kwon@uci.edu

Abstract—Among ML operators today, GeneralMatrix Multiplication (GEMM)-based operators are known to be key operators that build the main backbone of ML models. As their computational overhead dominates the overall execution time (e.g., 42.8% - 96.6% in our results), GEMM operators have been the prime optimization targets for fast ML inference. This led to advanced GPUs and accelerators available today, which provided significant boost in the GEMM performance compared to CPUs, aligned with the lesson from Amdahl’s law. However, accelerating GEMM has significantly shifted the Amdahl’s law’s landscape for ML inference; due to the decreased GEMM execution time, the relative execution time of non-GEMM operators is not dominant. Although the importance of non-GEMM performance is increasing, we have little knowledge about the non-GEMM performance horizon in the latest hardware platforms and models.

Therefore, to guide non-GEMM-oriented optimizations, we conduct a thorough performance analysis of 16 widely adopted ML models in Hugging Face and Torchvision on workstation and data center platforms with/without GPUs. We discover that non-GEMM performance bottleneck is a considerable issue across all the platforms and models, accounting for 11.3% to 73.6% of total latency, on average. The challenge significantly aggravates when we apply quantization, which is a common model compression technique, due to the boosted GEMM performance and extra non-GEMM operators for dequantization and requantization. To provide insights into non-GEMM optimization targets, we demystify the most dominant non-GEMM operators for each model and deployment software. We also show that widely adopted optimizations such as operator fusion do not completely address the non-GEMM performance bottleneck, where non-GEMM operators still account for 15% to 48% of total latency. We will open-source our non-GEMM-oriented benchmark framework to facilitate research in non-GEMM optimization.

I. INTRODUCTION

The success of machine learning (ML) in various problem domains, such as computer vision (CV) [21], [22], [32], [37], [54] and natural language processing (NLP) [4], [31], [58], made ML workloads pervasive in various computing platforms from edge to cloud devices. ML model inference involves billions of multiply-and-accumulate (MAC) operations (e.g., 497 billions of MAC operations for ResNet 50 [22]). Such MAC operations originate from General Matrix Multiplication (GEMM)-based operators, such as CONV2D, Linear, and BMM (batched matrix multiplication). The GEMM-based operators dominate in terms of the total execution time on CPUs, as

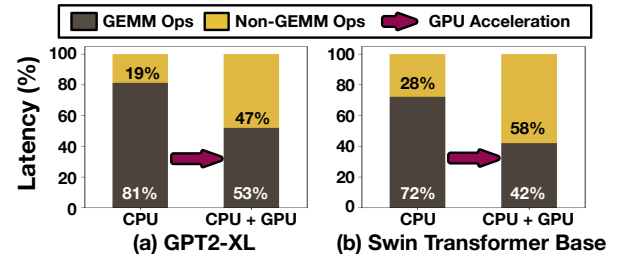


Fig. 1. The latency breakdown into GEMM and non-GEMM operators on AMD EPYC 7763 + NVIDIA A100 GPU. We measure the latency on two popular models from HuggingFace (a) GPT2-XL (batch 1) [4] and (b) Swin Transformer (batch 1) [37].

shown in Figure 1. Therefore, GPUs and accelerators have focused on the optimization of the GEMM-based operators, which significantly enhanced the computational performance (e.g., latency and throughput) of end-to-end ML model inference, as highlighted in Figure 1.

However, because the GEMM operators are being accelerated, the non-GEMM operators, such as memory operations (e.g., reshape, view, and transpose), normalization, and logit computation functions (e.g., Softmax), now account for a considerable amount of the end-to-end latency, compared to that of GEMM operators. Figure 1 shows the profiled latency breakdown into GEMM and non-GEMM operators running inferences on state-of-the-art large language (GPT2-XL [4]) and image classification (Swin Transformer [37]) models. The motivational data imply a major shift of the landscape of Amdahl’s law [24] for ML inference acceleration, indicating that we now need to consider non-GEMM operators as one of the major optimization targets in the ML system optimization. However, the research community today lacks a thorough and systematic performance analysis and characterization of non-GEMM operators in the latest models, which hinders the development of non-GEMM oriented optimization techniques.

Therefore, we collect widely-used ML models from Hugging Face [61] and Torchvision [38] and perform a thorough performance characterization of non-GEMM operators in the 18 latest models of four major task domains: Image Classification (IC), Image Segmentation (IS), Object Detection (OD), and Natural Language Processing (NLP). We evaluate the effect of GPU acceleration on the relative latency across

GEMM and non-GEMM operators in collected models and conduct deep-dive analysis on the impact of different hardware platforms (mobile, workstation, and datacenter), deployment software, and common optimizations (operator fusion and quantization). Based on our case studies, we highlight that the non-GEMM performance challenge is common in accelerated inferences and existing optimization techniques (e.g., operator fusion) cannot completely address the challenges. Also, we demystify the most time-consuming non-GEMM operators in each model, which will help the research community identify non-GEMM operators to be optimized.

To facilitate such research in non-GEMM-oriented optimization techniques, we build an open-source benchmark specialized in non-GEMM performance analysis, **NONGEMM BENCH**, which will be released after publication. **NONGEMM BENCH** can profile arbitrary non-GEMM operators supported by PyTorch [46], ONNX [7], and TensorRT [43], in addition to the preset of non-GEMM operators collected from the selected 16 popular models, which provides desired flexibility to users for follow-up research.

We summarize our contributions as follows:

- We shed a light on the changed landscape of Amdahl’s law in ML system design, which shows the increased importance of non-GEMM operators in systems with GEMM accelerations.
- We perform case studies on two different hardware configurations, workstation and data center, and show the non-GEMM operators are becoming a major consideration across all platforms.
- We identify different dominant non-GEMM operators depending on the model and deployment software flow, which indicates that non-GEMM optimization need to be specialized for each model and deployment software.
- We analyze the impact of a common non-GEMM-aware optimization, operator fusion and show that operator fusion does not completely mitigate non-GEMM bottleneck for all models, which motivates follow-up research in non-GEMM performance optimizations
- We evaluate the performance of non-GEMM operators with quantization and show the non-GEMM bottleneck aggravates with data.
- We will open-source **NONGEMM BENCH**, an expandable benchmark flow that enables thorough non-GEMM performance characterization for any model supported by ONNX runtime, Tensor RT, and PyTorch, to facilitate non-GEMM-oriented research.

II. BACKGROUND

A. ML Operators

ML operators are the building blocks for ML models, which define the computation over one or multiple input tensors. Examples include convolution (Conv2d), matrix multiplication (linear, BMM, etc.), activation, and normalization, as listed in Figure 2. We categorize operators into two classes: GEMM operation-based and the others, which we term as non-GEMM operators. We discuss each class of ML operators next.

1) *GEMM-based Operators (GEMM Operators)*: GEMM-based operators (or *GEMM operators*) refer to all the ML operators that can be represented as a matrix multiplication operation, which include linear, Conv2d, and batched-matrix multiplication (BMM). For example, Figure 2 (a) and (c) illustrate two popular GEMM operators: Linear and Conv2d operators, respectively. Each operator can be represented into a perfectly nested loop with multiply-and-accumulate (MAC) operation in the inner-most loop. Note that variants that are not matrix multiplication in the default form like Conv2d can be converted into GEMM (e.g., `im2col` [11]), which motivated the term, GEMM operator.

GEMM-based operators are known to be compute-intensive, which accounts for the majority of the execution unless accelerated by GPUs or accelerators, as CPU results in Figure 1 show. However, they have regular computation patterns that can be summarized as a perfectly nested for loop. The regular pattern allows various loop optimization techniques such as loop reordering, tiling, and parallelization, which is referred to as dataflow [33], [45], [66]. With the dominance of GEMM operators in execution time and high optimization potential together, GEMM operators have been the prime optimization target for acceleration, which led to high-performance GPUs (e.g., H100 [13]) and accelerators [29].

2) *Non-GEMM Operators*: Non-GEMM operators refer to all ML operators other than GEMM operators. They span various functionalities (e.g., memory layout manipulation and normalization) other than applying weights to input tensors. Because of their diverse functionalities, their computation patterns are often not a perfectly nested loop with MAC, which can also involve non-linear functions and memory-oriented operations. For example, Figure 2 (b) shows non-maximum suppression (NMS) operator often found in R-CNN model variants [21], [53]. As found in the example, the entire operation cannot be summarized into single perfectly-nested loop, which involve other operations such as sort and filtering. In addition, the operation involves a conditional statement, which introduces non-deterministic behaviors to the operator. The layer normalization example in Figure 2 (b) also shows another key characteristic of the non-GEMM operators: non-linear functions. Because of such characteristics distinguished from GEMM operators, optimization methodologies for GEMM operators cannot be applied to accelerate non-GEMM operators.

To understand the extent of the non-GEMM operators, we analyze non-GEMM operators in 16 recent models in the computer vision and natural language processing domains. We select models based on their popularity in the Hugging Face to obtain realistic workload. We list the models we investigated in Table I. Based on our analysis, we categorize non-GEMM operators based on their functionality and summarize their usage in models and characteristics in Table II.

- **Normalization**. Normalization operators regularize the data range across a selected dimension using the mean and standard deviation. Examples include Batch-Norm [26] and LayerNorm [6], which are widely adopted

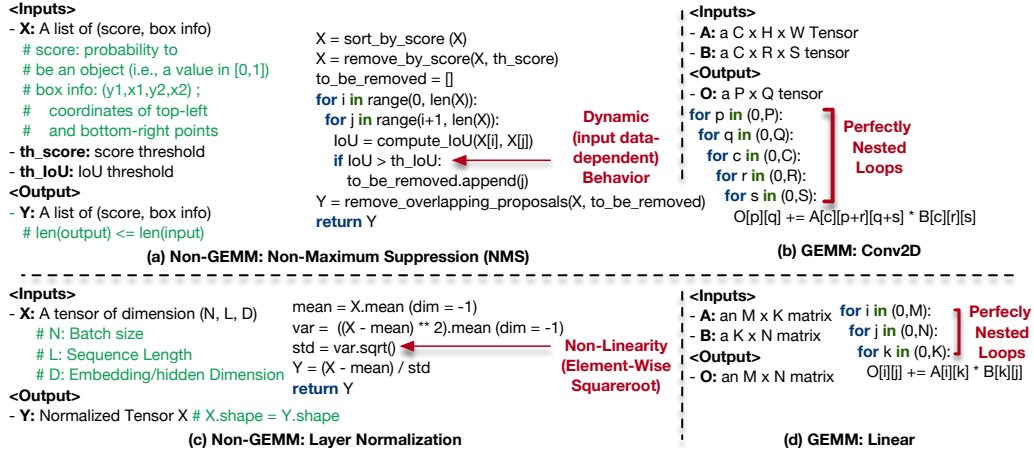


Fig. 2. A description of Linear (a) and Conv1D (c) operators as GEMM operators example, and that of non-maximum suppression [21] (b) and Layer Normalization [6] (d) as a non-GEMM operator example.

in computer vision and NLP models [4], [21]. RMS Norm [67], which is adopted in recent large language models [58], is another example of the normalization function. RMS Norm eliminates the division by standard deviation in typical normalization functions and performs $\sqrt{\frac{1}{n} \sum_{i=1}^n (X_i - \mu)^2}$, where X_i , n , and μ refer to the i -th data, number of data, and the mean, respectively.

- **Activation.** Activation operators introduce non-linearity into the model. Rectified Linear Unit (ReLU) function [41] is an example of activation operators used in CNN based ML models [22], [54], [55]. It injects non-linearity into the model based on the sign of the data by applying the function $X_i = \text{Max}(0, X_i)$ element-wise to the data, where X_i is the i -th data point. Another variant of activation operators is the the Gaussian Error Linear Units function (GELU) [23] which is a popular activation function adopted in transformer based ML models [4], [32], [37], [64]. Unlike ReLU, GELU accounts for the value of the data when inserting the non-linearity and not only the sign. It multiplies the input X_i by the Cumulative Distribution Function (CDF) of a Gaussian distribution: $\text{GELU}(X_i) = X_i * \phi(X_i)$ [23] where X_i is the i -th data and ϕ is the CDF of the Gaussian distribution.
- **Memory Operators.** Memory operators are responsible for the memory allocation and the layout modification of tensors. For example, Reshape modifies the shape (e.g. dimension order) of a tensor and return a new view of the tensor following the new dimension order.
- **Element-Wise Arithmetic.** Element-wise arithmetic operators cover non-GEMM operators applied on individual elements in a tensor. For example, Figure 3 (c) contains an element-wise division applied to scale the elements of tensors in the attention block
- **RoI Selection.** RoI selection operators are found in R-CNN variant detection models. [21], [53]. They filter down bounding boxes proposed by the region proposal network (Figure 3 (b)) and align the remaining boxes to the objects detected in the image. Non-Maximum

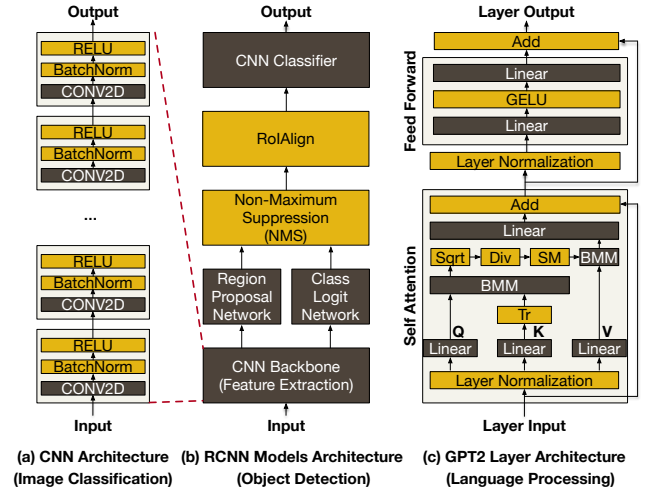


Fig. 3. Architectures of three popular ML model families.

Suppression (NMS) is an example of RoI Selection, which is described in Figure 2. Given a list of scores and bounding box information, it selects bounding boxes by applying the Intersection over Union (IoU) metric.

B. ML Models and Popular Tasks

The heterogeneity in non-GEMM operators enabled ML developers to build models supporting a wide range of tasks (e.g. Computer Vision and NLP). As highlighted in Figure 3, computer vision (Figure 3 a and b) and NLP (Figure 3) models are characterized by distinct architectures leveraging unique combinations of GEMM and non-GEMM operators.

For example, classical models in image classification shown in Figure 3 (a) consist of deep convolution networks (CNN), which cascade Conv2d (GEMM) with normalization and activation operators [22], [54]. Object Detection models also rely on convolution network for feature extraction, region proposal and classification. However, they pair the CNNs with ROI selection non-GEMM operators to process and filter the detections (Figure 3 (b)). On the other hand, NLP and language models rely on the transformer architecture,

which leverages the attention mechanism introduced in [59]. Transformers combine BMMs and Linear GEMM operators with normalization, memory and arithmetic non-GEMM operators as shown in Figure 3. This diversity in non-GEMM operators and model architectures across tasks paired the preliminary data presented in Figure 1 motivate us to study the impact of non-GEMM operators have on the inference performance of popular models.

III. PERFORMANCE CHARACTERIZATION METHODOLOGY

To understand the realistic performance landscape of the latest ML models with non-GEMM workloads, we must (1) capture operator level performances in end-to-end inferences to understand, (2) use widely-used models by the research community and industry, (3) cover diverse task domains, and (4) use real datasets.

However, ML Benchmarks available today (e.g., MLPerf [52]), unfortunately, do not satisfy all the requirements since they do not focus on the non-GEMM operators. Long-tail bench [34] identified a similar problem as this work, but it focuses on a limited set of custom kernels, which fails to represent broad task domain. Therefore, to facilitate our non-GEMM operators analysis and better-understand the impact of non-GEMM operators on system performance, we develop a new ML benchmark, NONGEMM BENCH. NONGEMM BENCH provides operator-level breakdown of end-to-end inference latency in the operator graph level, which enables detailed non-GEMM operator performance analysis, as we present in Section IV. To capture the performance in the latest ML workload, we select 15 highly downloaded (more than 10K downloads on average) models from HuggingFace [1] to enhance the *representativeness* of NONGEMM BENCH and our analysis. We discuss the datasets and models in NONGEMM BENCH in detail and describe the structure of NONGEMM BENCH next.

A. Evaluated Models

Table I lists the NONGEMM BENCH model registry which contains 15 models based on state-of-the-art CNN and Transformer architectures with number of parameters ranging from 0.85M to 7B, demonstrating the *diverse* model coverage of NONGEMM BENCH. The selected models cover four major task domains in ML, which include Image Classification (IC), Object Detection (OD), Image Segmentation (IS), and Natural Language Processing (NLP).

1) *Computer Vision (CV)*: Deep learning is widely used in the CV domain [32] [22] [53]. NONGEMM BENCH covers three important tasks in the domain:

Image Classification (IC). Image classification refers to a CV task that identifies a class label of a given image. Image classification models extract features (i.e., high-level and dimensional information of the input image) from an input image and report the class label utilizing the features. NONGEMM BENCH includes eight most popular IC models in HuggingFace [1]: Three variants of Vision Transformer [32], and three variants of Swin Transformer [37].

Image Segmentation (IS). Image segmentation refers to a computer vision task that identifies the area in a image for each class. Like IC models, IS models also extract features and utilize them to identify objects located in an image and spatially separate them by highlighting pixels that belong to each object. NONGEMM BENCH includes two state-of-the-art IS models: Segformer [64] and MaskFormer [10]. **Object Detection (OD).** Object detection refers to a computer vision task that identifies the location of objects in an image and outputs the bounding box of each object. OD models extract features and generate region proposals, which refer to the candidate locations and bounding boxes of objects. Using Region of Interest (RoI) processing non-GEMM operators in Table II, OD models refine raw region proposals generated by a region proposal network. The refined RoIs are used as inputs to the CNN classifier at the end, and the classifier determines the class label of objects inside each refined RoI. NONGEMM BENCH includes three popular OD models [2]: FasterRCNN [53], MaskRCNN [21], and DETR [9].

2) *Natural Language Processing (NLP)*: NLP refers to tasks involving the analysis and understanding of human (natural) language. NLP models extract context and features from an input text sequence and use the extracted context and features to perform multiple applications like translation and text generation [68] [8]. Transformer [59] based DNNs have become the dominant model architecture in NLP and are the backbone of popular state-of-the-art generative large language models like GPT [50] and Llama [58]. Figure 3 (c) shows the layer architecture of GPT’s transformer. It consists of a self-attention block built by cascading GEMM operators with Normalization, Memory, Logit Computation and Element-wise Arithmetic non-GEMM operators (Table II). NONGEMM BENCH includes five popular NLP models [3]: Bert [31], three variants of GPT2 [4], and Llama2-7b [58].

B. Profiling Methodology

To enable the thorough analysis of the landscape of non-GEMM performance presented in Section IV, NONGEMM BENCH provides an end-to-end profiling flow to breakdown the inference latency at the operator level. We discuss input, output, and the benchmark software structure.

1) *NONGEMM BENCH Inputs*: NONGEMM BENCH receives target deployment software flow (PyTorch, ONNX runtime, or TensorRT), dataset, and other configurations listed in Figure 4 as inputs. Optionally, users can provide custom models with associated datasets to profile their workloads. By default, NONGEMM BENCH runs the 15 models in Table I. We describe each input in detail as follows.

Models. As described in Section III-A, NONGEMM BENCH includes a registry of 15 selected popular ML models. Nonetheless, we designed NONGEMM BENCH to be easily expandable to accommodate rapidly evolving ML models that constantly introduce new operators. Users can benefit from the features of our benchmark by simply plugging their new models into the NONGEMM BENCH model registry (Figure 4) by specifying the model class, its weights and any data preprocessor.

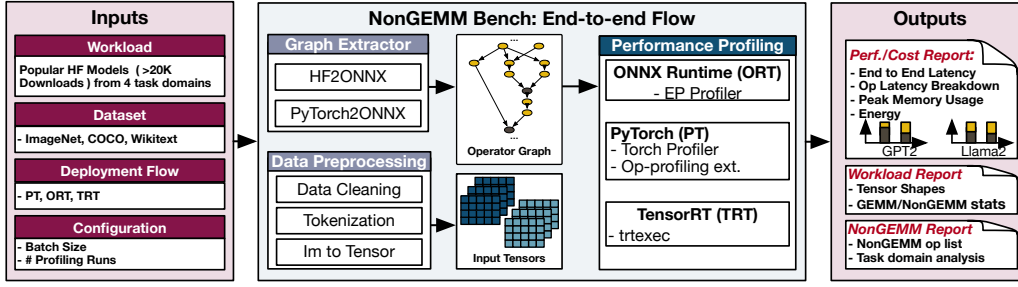


Fig. 4. An overview of NONGEMM BENCH flows

TABLE I
TASKS AND MODELS EVALUATED IN SECTION IV

Application	Models	# Params	Dataset
Image Classification (IC)	ViT base (Vt-b) [32]	307M	ImageNet [15]
	ViT large (Vt-l) [32]	307M	
	ViT huge (Vt-h) [32]	632M	
	Swin tiny (Sw-t) [37]	29M	
	Swin small (Sw-s) [37]	50M	
	Swin base (Sw-b) [37]	88M	
Object Detection (OD)	FasterRCNN (FRCNN) [53]	42M	COCO [36]
	MaskRCNN (MRCNN) [21]	44M	
	DETR [9]	41M	
Image Segmentation (IS)	Maskformer (MF) [10]	102M	COCO [36]
	SegFormer (Seg) [64]	3.7M	
Natural Language Processing (NLP)	GPT2 [4]	117M	wikitext [39]
	GPT2 Large (gpt2-l) [4]	762M	
	GPT2 X-Large (gpt2-xl) [4]	1.5B	
	Llama 2-7B [58]	7B	
	Bert [31]	110M	

Deployment Flow. NONGEMM BENCH deploys its models using three popular inference frameworks: ONNX Runtime [17], PyTorch [46] TensorRT [43].

Datasets. To evaluate the models, NONGEMM BENCH utilizes real data from popular datasets in each domain. We use ImageNet 2012 [15] and MS COCO [36] for computer vision tasks. As for language models, we use wikitext dataset [39] available on HuggingFace. For custom models, users can specify their own dataset for the model.

Misc. Configurations. This includes the batch size, the number of profiling iterations, and the target device.

2) *End-to-End Inference Flow:* The end-to-end inference flow profiles NONGEMM BENCH models running inferences on data samples from the selected dataset.

First, the *Graph Extractor* extracts the operator graph of a given model based on the selected deployment flow. NONGEMM BENCH calls graph exporters from the HuggingFace transformers library [62] or from the PyTorch libraries. Second, model specific *Data Preprocessing* functions fetch the raw data from the specified dataset, clean the data, and apply tokenization or image to tensor transformations to generate input tensors for the profiling stage.

Third, *End-to-End Inference Profiling* functions run the profiling iterations on the received the model and its inputs. The profiling functions are deployment flow specific. For ONNX Runtime, we invoke Execution Provider profiling in the inference session. Currently, we only support operator level profiling for CPU and CUDA execution providers [17] because profiling support to other ONNX RUNTIME backends is not

stable yet. For PyTorch, we use the PyTorch Profiler [49]. For TensorRT, we leverage the TensorRT open source software framework profiling APIs [44].

3) *NONGEMM BENCH Outputs:* NONGEMM BENCH generates many statistics organized into three categories: performance, workload, and non-GEMM-specific reports. The performance report includes key performance metrics such as the end-to-end latency with operator level break-downs and peak memory usage. The workload report includes the types of operators and the shape of the tensors for each operator captured during inference on realistic data. Finally, the non-GEMM report provides insights on non-GEMM operators, such as the number of operator variants of the same class of non-GEMM operator (e.g., layernorm implementation could have multiple variants for each ML framework) and non-GEMM operator trace on different domains.

IV. CASE STUDIES

We perform a thorough performance analysis of models in Table I on multiple hardware platforms listed in Table III. The evaluated hardware platforms span workstation and data center-class CPUs and GPUs. We employ PyTorch, ONNX runtime, and TensorRT as deployment flows to investigate their impact on the performance horizon.

Using the aforementioned workload, hardware platforms, and deployment flow, we characterize the GEMM/non-GEMM performance for each model in NONGEMM BENCH and investigate the impact of the hardware platform and deployment flow. In addition, we also investigate the impact of widely adopted optimizations (operator fusion and quantization) and show that the non-GEMM performance is an issue even after applying common optimizations.

A. Non-GEMM Performance Characterization Results

We first conduct a performance characterization study using PyTorch and present the characterization results on datacenter and workstation platforms (Platforms A and B in Table III) in Figure 5. We focus on those two platforms since some models (e.g, large language models) do not fit into the mobile devices. As expected, the relative contribution of non-GEMM operators to the end-to-end latency significantly increases after GPU acceleration, on average, from 17.2% to 42.3%. However, we observe each model show different trends,

TABLE II
NON-GEMM OPERATORS IN EIGHT SELECTED MODEL VARIANTS FROM TABLE I AND THEIR CHARACTERISTICS.

Operator Group	Operator	Model	Single Operation	Single Operand	Non Linearity	Dynamicity	Reduction	Example Input Shape
Activation	ReLU	DETR	✓	✓				[2,64,533]
	GELU	ViT-l16		✓	✓			[1, 97, 4096]
	GELU	GPT2-XL		✓	✓			[1, 8, 6400]
	SiLU	Llama-2		✓	✓			[1, 10, 11008]
Normalization	LayerNorm	Segformer		✓	✓		✓	[2, 16384, 32]
	BatchNorm2d	Segformer		✓	✓		✓	[2, 256, 128, 128]
	LlamaRMSNorm	Llama		✓	✓		✓	[1, 10, 4096]
	FrozenBatchNorm2d	MaskRCNN		✓	✓		✓	[1, 1024, 50,68]
	FrozenBatchNorm2d	DETR		✓	✓		✓	[1, 2048, 25, 34]
Elmt-wise Arithmetic	LayerNorm	DETR		✓	✓		✓	[2, 850, 256]
	Add	Segformer	✓					[2, 16384, 32]
	Mul	Llama-2	✓					[1, 10, 11008]
	Neg	Llama-2	✓					[1, 32, 10, 64]
	TrueDiv	Segformer	✓					[2, 1, 16384, 256]
	TrueDiv	GPT2-XL	✓					[1, 25, 8, 8]
Memory	Contiguous	Segformer	✓	✓				[2, 32, 128, 128]
	Contiguous	Llama-2	✓	✓				[1, 10, 32, 128]
	Permute	ViT-b16	✓	✓				[1, 768, 196]
	Permute	GPT2-XL	✓	✓				[1, 8, 25, 64]
	Split	GPT2-XL	✓	✓				[1, 8, 4800]
	View	GPT2-XL	✓	✓				[1, 8, 1600]
	Reshape	ViT-b16	✓	✓				[1, 768, 14, 14]
	Expand	ViT-b16	✓	✓				[1, 1, 768]
	Squeeze	Llama-2	✓	✓				[1, 1, 10, 128]
Logit Computation	Softmax	DETR	✓	✓	✓		✓	[1, 25, 8, 8]
	Softmax	Segformer	✓	✓	✓		✓	[2, 1, 16384, 256]
RoI Selection	NMS	MaskRCNN				✓		[4663, 4]
Interpolation	Interpolate	Segformer		✓				[2, 256, 128, 128]

TABLE III
HARDWARE PLATFORM CONFIGURATIONS USED FOR CASE STUDIES.

ID	Class	CPU	GPU		
		Device	Device	Mem.	TOPS
A	Datacenter	AMD EPYC 7763	Nvidia A100	80 GB	624
B	Workstation	Intel i9-13900K	Nvidia RTX 4090	24 GB	660

mainly affected by the non-GEMM operator types and the number of GEMM and non-GEMM operators in the original model. We summarize the most time-consuming non-GEMM operators in Table IV from the datacenter class platform (Platform A), which shows the diversity of the dominating non-GEMM operators in each model. We highlight some notable models in each task category and delve into the details of their non-GEMM performance.

IC Task: Swin Transformer. For every Swin Transformer variant (Sw-t, -s, and -b), the memory operator group is the most latency-dominant non-GEMM operator group, which accounts for 32% of the total latency, on average, on data center platform with GPU acceleration. Those memory operators originate from the Swin Transformer’s unique window shape (cross-shaped) [37], which is not well-aligned with memory layout of tensor data organized in dimension orders.

OD Task: DETR. After GPU acceleration, DETR has shown significant non-GEMM operator presence, which accounts for 65.8% of the total latency, on average. The major source of the non-GEMM latency is in the normalization operators, whose percentages are 35% and 32% on Platforms A and B, respectively. We observe the normalization functions are based on a custom implementation, which are identified as independent kernel. Kernel launch overheads accumulated for independent runs for the custom normalization function significantly contribute to the non-GEMM latency. However,

TABLE IV
MOST TIME-CONSUMING NON-GEMM OPERATOR GROUPS FOR SELECTED MODELS (PLATFORM A, WITH GPU ACCELERATION, AVERAGE ACROSS BATCH SIZES).

Task Domain	Model	Operator Group	Latency Percentage (%)
Image Classification	Vt-b	Norm	14.0
	Vt-l	Norm	13.3
	Vt-h	Norm	11.2
	Sw-t	Memory	31.8
	Sw-s	Memory	33.1
	Sw-b	Memory	32.8
Object Detection	FRCNN	Elmt-wise Arith.	34.4
	MRCNN	Elmt-wise Arith.	33.6
	DETR	Norm	34.8
Image Segmentation	MF	Memory	40.8
	Seg	Normalization	17.4
NLP	gpt2	Act	30.2
	GPT2-L	Act	29.9
	GPT2-XL	Act	28.1
	Llama2	Norm	14.9
	bert	Norm	13.1

we also observe that an advanced deployment software (TensorRT) can fuse those operators and significantly improve the non-GEMM performance. We discuss the details later in Section IV-B.

IS Task: Maskformer. MaskFormer utilizes Swin Transformer as its backbone, which introduces many memory operators as we discussed for Swin Transformer. As a result, memory operator is the dominant non-GEMM operator, which accounts for 40.8% of the total latency, on average, as we can observe in Figure 5 (f) and (n).

NLP Task: GPT2. The latencies of non-GEMM operators in GPT2 variants are considerable, which account for 45.0%, on average, as we observe in Figure 5 (h) and (p). The dominant non-GEMM operator is activation, GELU, which required 26.4% of the total latency.

Summary. We observe GPU acceleration significantly increase the percentage of non-GEMM operators and increase the importance of non-GEMM operators in performance optimization. Also, the dominant operators are diverse in each model, which indicates an optimization technique tailored for a single operator cannot fully address the non-GEMM performance problem.

B. The Impact of Deployment Flow on Non-GEMM Performance

Deployment flows such as ONNX runtime [17] and TensorRT [43] are widely used for serving model inferences. Such flows apply various optimizations to each model, which includes the computational graph level optimizations (e.g., operator fusion) and backend assignment (e.g., utilizing Tensor Core in Nvidia GPUs). To understand the effect of deployment frameworks on the operator performance, we conduct two case studies (1) comparing PyTorch and ONNX Runtime (ORT) results on LLMs (focus: general optimizations w/o operator fusion) on LLMs, and (2) comparing PyTorch and TensorRT results (focus: operator fusion).

1) *Case Study 1: Non-GEMM Performance on LLMs across PyTorch and ORT:* We run two LLMs (GPT2 and Llama2) using the CUDA execution provider in ORT and compare their non-GEMM performance percentage in Figure 6.

In the results, we observe the presence of non-GEMM operators significantly increase, from 52.6% to a 80.75%, on average. We observe the percentage of memory operators significantly amplifies after applying ORT, from 3.2% to 66.8%. Such a result originates from the limitation in operator support in ORT. Many memory operators in the evaluated LLMs are not supported by the cuda execution provider in ORT, which leads to inefficient execution on CPUs involving data transfer between a CPU and a GPU. Combined with the high frequency of those operators, the inference latency of memory operators increases significantly, as shown in Figure 6 (b). The results imply two insights: (1) Model deployment flow can significantly aggravate the non-GEMM performance challenge and (2) the dominant non-GEMM operators differ depending on the operator support in a deployment flow.

2) *Case Study 2: Non-GEMM Performance with Operator Fusion:* Operator fusion is a key optimization technique for accelerating inference workloads [14], [25], [30], [42], [43], [57]. Fusion combines multiple operators in a single kernel to reduce the number of costly kernel launches and minimize the number of redundant offchip memory accesses [42]. TensorRT [43] is a widely adopted inference framework released by Nvidia that applies the operator fusion technique targeting GPUs. Operator fusion in TensorRT detects specific patterns (e.g., three consecutive element-wise operators [43]) in the operator graph and fuses nodes captured in the patterns to enhance inference performance by reducing redundant memory accesses around non-GEMM operators.

Impact of Operator Fusion. To understand the impact of operator fusion on non-GEMM performance horizon, we

conduct a case study on four models, which compares the TensorRT (with fusion) and PyTorch (without fusion). We present the results in Figure 7, which shows the inference latency breakdown between GEMM and non-GEMM operators. We notice that fusion does not completely address the non-GEMM bottleneck in Swin-b model. For example, the percentage of non-GEMM operators in the total latency changes from 56.2% to 32.2%, on average, after operator fusion by TensorRT. The reduction in the percentage is based on the improvement of non-GEMM performance via operator fusion, which reduces 88.6% of latency after fusion, as summarized in Table V. However, the non-GEMM operators still account for 32.2% of total latency, which is considerable. This shows that operator fusion cannot eliminate the non-GEMM performance challenge and motivates further studies toward non-GEMM performance.

Factors Affecting the Effectiveness of Fusion. Although most results indicate considerable impact of non-GEMM even after operator fusion, we observe operator fusion on DETR model is exceptionally effective. Therefore, we conduct a deep-dive study, investigating the percentage of fused non-GEMM operators (i.e., fusion rate) and performance improvements after fusion, as listed in Table V. We observe the strong non-GEMM performance improvements for DETR originates from high fusion rate of 30%, which led to $13.5\times$ non-GEMM speedup. This leads to the large percentage reduction of non-GEMM in the total latency, from 67% to 18.5%, on average.

However, the fusion rate is not the only factor that determines the non-GEMM speedup. For example, DETR and Segformer have similar fusion rates (30% and 27%, respectively), but the amount of non-GEMM performance improvements are significantly different: $13.5\times$ and $2.39\times$, respectively. We analyze the execution trace and find that batch normalization is the main source of the differences. The main difference is the fusion pattern: most batch normalization operators (100% of total) in DETR were fused with GEMM-operators (CONV+BN+ReLU pattern) while those in Segformer were fused with other non-GEMM operators (97.8% of total). The results indicate that the effectiveness of operator fusion relies on not only the overall fusion rate but also the fusion patterns. Our observation confirms that the operator fusion cannot fully address the non-GEMM performance challenge, even if it can be very effective on some patterns.

C. Non-GEMM Performance with Quantization

Quantization refers to the model optimization technique, which reduces the bit precision of model weights and/or activations to enhance the computational performance and efficiency of DNN inference. Quantization is a widely-adopted technique [28], [40] including heavy models like LLMs [16], [19], [35], [63]. For example, LLM.int8() [16] introduced an 8-bit - 16-bit mixed precision quantization scheme for LLMs. LLM.int8() is a state-of-the-art quantization method, which quantizes more than 99% of the linear layers in OPT LLM to an 8-bit precision. Therefore, we adopt LLM.int8() and characterize GEMM and non-GEMM performance to

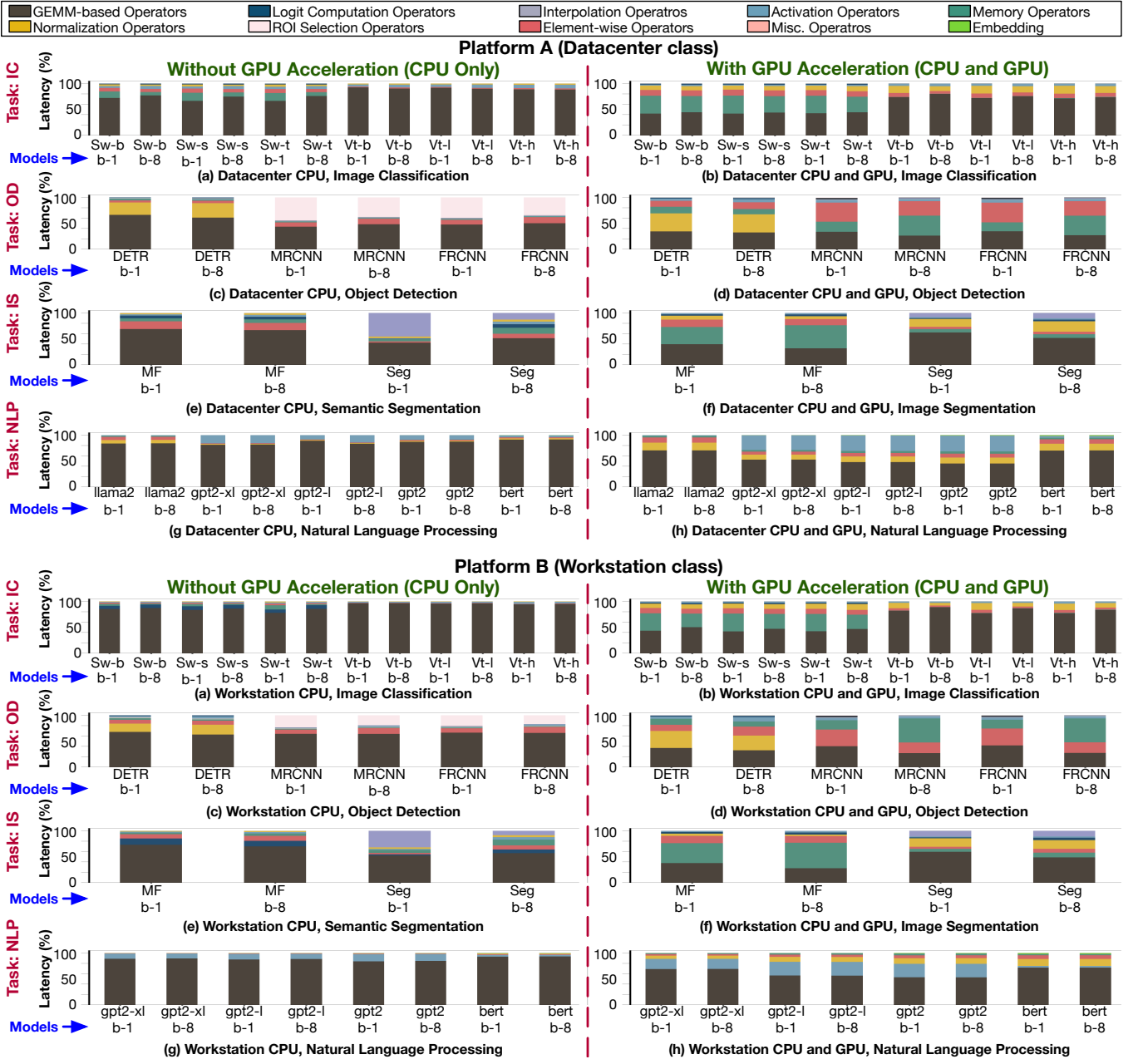


Fig. 5. Breaking down the execution time of models running on the Data Center (CPU only) and (CPU + GPU) configurations across operator groups.

understand the impact of quantization on the non-GEMM operator performance problem.

We conduct a case study on quantization using LLM.int8() on Llama3 LLM on the datacenter platform with GPU acceleration and present the results in Figure 8. In the results, we observe that non-GEMM operators dominate the latency after quantization, changing from 29.3% to 76.7%, on average. Such a significant shift in the latency distribution is mainly based on the GEMM performance improvements from 8-bit arithmetic, which reduced the latency by 38.2%, on average. However, based on our analysis on the execution traces, non-GEMM performance aggravates because the 8-bit data need to be dequantized and re-quantized for non-GEMM

operators, which requires 16-bit floating point arithmetic. This led to 6510 additional non-GEMM operators into the computational graph, which led to a significant increase of the non-GEMM latency by 5.6 \times after quantization. Combined together, the overall percentage of non-GEMM operators in the total latency dominate after quantization, which makes non-GEMM operators as the major optimization target.

In the case study on Llama3 8B, we observe the element-wise arithmetic operators originate from dequantization/requantization (DQRQ) process dominate in the inference latency, which adds 20% extra non-GEMM operators to the original computational graph. Also, we observe longer sequence length leads to higher percentage in the element-

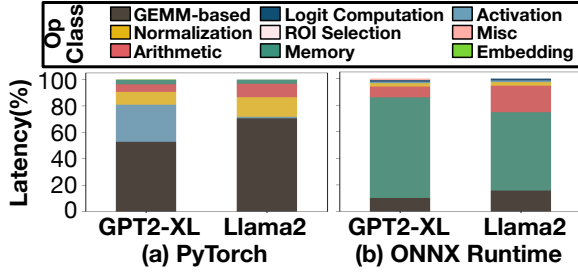


Fig. 6. The impact of deployment software toolchain into the latency breakdown on language models. (a) PyTorch and (2) ONNX Runtime on a data center class GPU (A100).

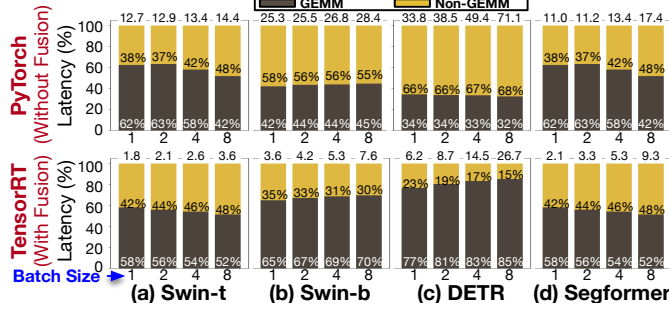


Fig. 7. The latency of non-GEMM operator in (a) Swin-b, (b) DETR, and (c) Segformer is still considerable despite applying operator fusion in TensorRT. The numbers at the top of each bar represent the latencies in milliseconds.

wise arithmetic operators. For example, as we increase the sequence length from 512 to 8192, the latency percentage of element-wise arithmetic operators increase from 31.8% to 63.8%. As current trends in the LLMs are toward longer sequence lengths [5], [18], the non-GEMM performance issues in longer sequences originating from DQRQ costs will aggravate, which motivates efforts in non-GEMM performance optimization.

D. Key Observations and Insights

We summarize our main observations and insights:

- After GEMM acceleration, non-GEMM becomes a major optimization target regardless of the hardware platforms.
- Specialized optimization for one non-GEMM is not effective due to the diversity in dominant non-GEMM.
- Operator fusion cannot fully address non-GEMM performance challenge: Although it can significantly improve non-GEMM performance, but its effectiveness heavily depends on the model.
- Operator support in deployment flows significantly affects the non-GEMM performance horizon.
- Quantization significantly aggravates the non-GEMM performance challenge due to the imbalanced speedup across GEMM and non-GEMM and quantization/dequantization costs around non-GEMM operators

V. RELATED WORKS

Previous works characterized ML workloads and non-GEMM operators. However, the main limitations are listed below: State-of-the-art inference benchmarks [20], [52] do not thoroughly analyze the performance of Non-GEMM operators. Other works characterizing non-GEMM operators focus on

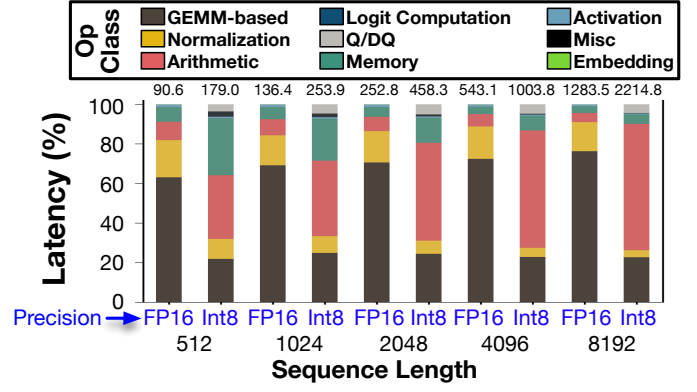


Fig. 8. Non-GEMM operators latency contribution to the inference of a quantized Llama3 8B using 8 bit quantization [16]. The numbers at the top of each bar represent the latencies in milliseconds.

TABLE V

THE NON-GEMM LATENCY BEFORE AND AFTER APPLYING FUSION WITH TENSORRT. THE VALUES BETWEEN BRACKETS REPRESENT THE PERCENTAGE W.R.T THE TOTAL INFERENCE LATENCY.

Model	Non-GEMM Fusion Rate	Non-GEMM Latency	
		Before Fusion	After Fusion
Swin-t	8.75%	7.53 ms (56.4%)	0.97 ms (39%)
Swin-b	7%	14.59 ms (58%)	1.65 ms (32.25%)
DETR	30%	32.17 ms (66.4%)	2.38 ms (18.5%)
Segformer	27%	5.57 ms (41%)	2.33 ms (41%)

a specific application domain [34], [47], [48], [65] for their non-GEMM study. In [48], [27], and [47] the authors analyze the performance of non-GEMM operators, however they focus on a specific class of transformer language models. Similarly, [34] only studies a limited number of operators from computer vision models in a microbenchmarking flow. Previous works that also studied non-GEMM operator performance bottlenecks [12], [51], [56], [60], mostly focused on softmax operators in transformers for language models. Our work extends on the pioneering efforts of these works by studying non-GEMM operators from 15 models covering 4 various task domains.

VI. CONCLUSION

Accelerating GEMM operators in ML inference is shifting the landscape of Amdahl's law to have more presence of non-GEMM operators in the performance horizon. In this paper, we conducted a thorough performance analysis of non-GEMM operators in the latest models in various task domains and platforms. The results confirm the increasing importance of non-GEMM performance and show model optimizations we apply (e.g., quantization) can significantly aggravate the non-GEMM performance challenge. The dominant non-GEMM operators are diverse across models, which indicates that a specialized optimization targeting a specific operator cannot solve the non-GEMM performance challenge. We also show that non-GEMM-oriented optimization such as operator fusion cannot fully address the non-GEMM performance challenge.

Our performance analysis results imply that now we need to consider non-GEMM operators as a major optimization

target and develop new hardware and software techniques to optimize non-GEMM performance. The non-GEMM profiling software we used in this study, NONGEMM BENCH, will be released as open-source software, which will contribute to such follow-up research.

REFERENCES

- [1] “Hugging face models hub,” <https://huggingface.co/models>, accessed on March 8, 2024.
- [2] “Hugging face models hub - object detection,” https://huggingface.co/models?pipeline_tag=object-detection&sort=downloads, accessed on March 8, 2024.
- [3] “Hugging face models hub - text generation,” https://huggingface.co/models?pipeline_tag=text-generation&sort=downloads, accessed on March 8, 2024.
- [4] J. Achiam, S. Adler, S. Agarwal, L. Ahmad, I. Akkaya, F. L. Aleman, D. Almeida, J. Altenschmidt, S. Altman, S. Anadkat *et al.*, “Gpt-4 technical report,” *arXiv preprint arXiv:2303.08774*, 2023.
- [5] —, “Gpt-4 technical report,” *arXiv preprint arXiv:2303.08774*, 2023.
- [6] J. L. Ba, J. R. Kiros, and G. E. Hinton, “Layer normalization,” *arXiv preprint arXiv:1607.06450*, 2016.
- [7] J. Bai, F. Lu, K. Zhang *et al.*, “Onnx: Open neural network exchange,” <https://github.com/onnx/onnx>, 2019.
- [8] T. Brown, B. Mann, N. Ryder, M. Subbiah, J. D. Kaplan, P. Dhariwal, A. Neelakantan, P. Shyam, G. Sastry, A. Askell *et al.*, “Language models are few-shot learners,” *Advances in neural information processing systems*, vol. 33, pp. 1877–1901, 2020.
- [9] N. Carion, F. Massa, G. Synnaeve, N. Usunier, A. Kirillov, and S. Zagoruyko, “End-to-end object detection with transformers,” in *European conference on computer vision*. Springer, 2020, pp. 213–229.
- [10] B. Cheng, A. Schwing, and A. Kirillov, “Per-pixel classification is not all you need for semantic segmentation,” *Advances in Neural Information Processing Systems*, vol. 34, pp. 17 864–17 875, 2021.
- [11] S. Chetlur, C. Woolley, P. Vandermersch, J. Cohen, J. Tran, B. Catanzaro, and E. Shelhamer, “cudnn: Efficient primitives for deep learning,” *arXiv preprint arXiv:1410.0759*, 2014.
- [12] J. Choi, H. Li, B. Kim, S. Hwang, and J. H. Ahn, “Accelerating transformer networks through recomposing softmax layers,” in *2022 IEEE International Symposium on Workload Characterization (IISWC)*. IEEE, 2022, pp. 92–103.
- [13] N. Corporation, “Nvidia h100 tensor core gpu,” 2023. [Online]. Available: <https://www.nvidia.com/en-us/data-center/h100/>
- [14] T. Dao, D. Fu, S. Ermon, A. Rudra, and C. Ré, “Flashattention: Fast and memory-efficient exact attention with io-awareness,” *Advances in Neural Information Processing Systems*, vol. 35, pp. 16 344–16 359, 2022.
- [15] J. Deng, W. Dong, R. Socher, L.-J. Li, K. Li, and L. Fei-Fei, “ImageNet: A Large-Scale Hierarchical Image Database,” in *CVPR09*, 2009.
- [16] T. Dettmers, M. Lewis, Y. Belkada, and L. Zettlemoyer, “Llm.int8(): 8-bit matrix multiplication for transformers at scale,” in *Proceedings of the 36th International Conference on Neural Information Processing Systems*, ser. NIPS ’22. Red Hook, NY, USA: Curran Associates Inc., 2024.
- [17] O. R. developers, “Onnx runtime,” <https://onnxruntime.ai/>, 2021.
- [18] A. Dubey, A. Jauhri, A. Pandey, A. Kadian, A. Al-Dahle, A. Letman, A. Mathur, A. Schelten, A. Yang, A. Fan *et al.*, “The llama 3 herd of models,” *arXiv preprint arXiv:2407.21783*, 2024.
- [19] E. Frantar, S. Ashkboos, T. Hoefler, and D. Alistarh, “Gptq: Accurate post-training quantization for generative pre-trained transformers,” *arXiv preprint arXiv:2210.17323*, 2022.
- [20] Y. Hao, X. Zhao, B. Bao, D. Berard, W. Constable, A. Aziz, and X. Liu, “Torchbench: Benchmarking pytorch with high api surface coverage,” *arXiv preprint arXiv:2304.14226*, 2023.
- [21] K. He, G. Gkioxari, P. Dollár, and R. Girshick, “Mask r-cnn,” in *Proceedings of the IEEE international conference on computer vision (ICCV)*, 2017, pp. 2961–2969.
- [22] K. He, X. Zhang, S. Ren, and J. Sun, “Deep residual learning for image recognition,” in *Proceedings of the IEEE conference on computer vision and pattern recognition*, 2016, pp. 770–778.
- [23] D. Hendrycks and K. Gimpel, “Gaussian error linear units (gelus),” *arXiv preprint arXiv:1606.08415*, 2016.
- [24] M. D. Hill and M. R. Marty, “Amdahl’s law in the multicore era,” *Computer*, vol. 41, no. 7, pp. 33–38, 2008.
- [25] M. Hu, A. Venkatram, S. Biswas, B. Marimuthu, B. Hou, G. Oliaro, H. Wang, L. Zheng, X. Miao, J. Zhai, and Z. Jia, “Optimal kernel orchestration for tensor programs with korch,” in *Proceedings of the 29th ACM International Conference on Architectural Support for Programming Languages and Operating Systems, Volume 3*, ser. ASPLOS ’24. New York, NY, USA: Association for Computing Machinery, 2024, p. 755–769. [Online]. Available: <https://doi.org/10.1145/3620666.3651383>
- [26] S. Ioffe and C. Szegedy, “Batch normalization: Accelerating deep network training by reducing internal covariate shift,” in *International conference on machine learning*. pmlr, 2015, pp. 448–456.
- [27] A. Ivanov, N. Dryden, T. Ben-Nun, S. Li, and T. Hoefler, “Data movement is all you need: A case study on optimizing transformers,” *Proceedings of Machine Learning and Systems*, vol. 3, pp. 711–732, 2021.
- [28] B. Jacob, S. Kligys, B. Chen, M. Zhu, M. Tang, A. Howard, H. Adam, and D. Kalenichenko, “Quantization and training of neural networks for efficient integer-arithmetic-only inference,” in *Proceedings of the IEEE conference on computer vision and pattern recognition*, 2018, pp. 2704–2713.
- [29] N. P. Jouppi, C. Young, N. Patil, D. Patterson, G. Agrawal, R. Bajwa, S. Bates, S. Bhatia, N. Boden, A. Borchers *et al.*, “In-datacenter performance analysis of a tensor processing unit,” in *Proceedings of the 44th annual international symposium on computer architecture*, 2017, pp. 1–12.
- [30] S.-C. Kao, S. Subramanian, G. Agrawal, A. Yazdanbakhsh, and T. Krishna, “Flat: An optimized dataflow for mitigating attention bottlenecks,” in *Proceedings of the 28th ACM International Conference on Architectural Support for Programming Languages and Operating Systems, Volume 2*, 2023, pp. 295–310.
- [31] J. D. M.-W. C. Kenton and L. K. Toutanova, “Bert: Pre-training of deep bidirectional transformers for language understanding,” in *Proceedings of NAACL-HLT*, 2019, pp. 4171–4186.
- [32] A. Kolesnikov, A. Dosovitskiy, D. Weissenborn, G. Heigold, J. Uszkoreit, L. Beyer, M. Minderer, M. Dehghani, N. Houlsby, S. Gelly, T. Unterthiner, and X. Zhai, “An image is worth 16x16 words: Transformers for image recognition at scale,” in *Proceedings of the International Conference on Learning Representations (ICLR)*, 2021.
- [33] H. Kwon, P. Chatarasi, M. Pellauer, A. Parashar, V. Sarkar, and T. Krishna, “Understanding reuse, performance, and hardware cost of dnn dataflow: A data-centric approach,” in *Proceedings of the 52nd Annual IEEE/ACM International Symposium on Microarchitecture*, 2019, pp. 754–768.
- [34] X. Li, S. Yan, L. Jiang, P. Xu, J. Ma, X. Zhang, and D. Lin, “Longtail-bench: A benchmark suite for domain-specific operators in deep learning,” in *2022 IEEE International Symposium on Workload Characterization (IISWC)*. IEEE, 2022, pp. 282–295.
- [35] J. Lin, J. Tang, H. Tang, S. Yang, W.-M. Chen, W.-C. Wang, G. Xiao, X. Dang, C. Gan, and S. Han, “Awq: Activation-aware weight quantization for on-device llm compression and acceleration,” *Proceedings of Machine Learning and Systems*, vol. 6, pp. 87–100, 2024.
- [36] T.-Y. Lin, M. Maire, S. Belongie, J. Hays, P. Perona, D. Ramanan, P. Dollár, and C. L. Zitnick, “Microsoft coco: Common objects in context,” in *Computer Vision—ECCV 2014: 13th European Conference, Zurich, Switzerland, September 6–12, 2014, Proceedings, Part V 13*. Springer, 2014, pp. 740–755.
- [37] Z. Liu, Y. Lin, Y. Cao, H. Hu, Y. Wei, Z. Zhang, S. Lin, and B. Guo, “Swin transformer: Hierarchical vision transformer using shifted windows,” in *Proceedings of the IEEE/CVF international conference on computer vision (ICCV)*, 2021, pp. 10 012–10 022.
- [38] T. maintainers and contributors, “Torchvision: Pytorch’s computer vision library,” <https://github.com/pytorch/vision>, 2016.
- [39] S. Merity, C. Xiong, J. Bradbury, and R. Socher, “Pointer sentinel mixture models,” *arXiv preprint arXiv:1609.07843*, 2016.
- [40] M. Nagel, M. Fournarakis, R. A. Amjad, Y. Bondarenko, M. Van Baalen, and T. Blankevoort, “A white paper on neural network quantization,” *arXiv preprint arXiv:2106.08295*, 2021.
- [41] V. Nair and G. E. Hinton, “Rectified linear units improve restricted boltzmann machines,” in *Proceedings of the 27th international conference on machine learning (ICML-10)*, 2010, pp. 807–814.
- [42] W. Niu, J. Guan, Y. Wang, G. Agrawal, and B. Ren, “Dnnfusion: accelerating deep neural networks execution with advanced operator fusion,” in *Proceedings of the 42nd ACM SIGPLAN International Conference on Programming Language Design and Implementation*, 2021, pp. 883–898.
- [43] NVIDIA, “Nvidia tensorrt,” 2024, accessed: 2024-12-09. [Online]. Available: <https://developer.nvidia.com/tensorrt>

- [44] —, “Tensorrt github repository,” 2024, accessed: 2024-12-09. [Online]. Available: <https://github.com/NVIDIA/TensorRT>
- [45] A. Parashar, P. Raina, Y. S. Shao, Y.-H. Chen, V. A. Ying, A. Mukkara, R. Venkatesan, B. Khailany, S. W. Keckler, and J. Emer, “Timeloop: A systematic approach to dnn accelerator evaluation,” in *2019 IEEE international symposium on performance analysis of systems and software (ISPASS)*. IEEE, 2019, pp. 304–315.
- [46] A. Paszke, S. Gross, F. Massa, A. Lerer, J. Bradbury, G. Chanan, T. Killeen, Z. Lin, N. Gimelshein, L. Antiga *et al.*, “Pytorch: An imperative style, high-performance deep learning library,” *Advances in neural information processing systems*, vol. 32, 2019.
- [47] S. Pati, S. Aga, M. Islam, N. Jayasena, and M. D. Sinclair, “Tale of two cs: Computation vs. communication scaling for future transformers on future hardware,” in *2023 IEEE International Symposium on Workload Characterization (IISWC)*. IEEE, 2023, pp. 140–153.
- [48] S. Pati, S. Aga, N. Jayasena, and M. D. Sinclair, “Demystifying bert: System design implications,” in *2022 IEEE International Symposium on Workload Characterization (IISWC)*. IEEE, 2022, pp. 296–309.
- [49] PyTorch, “Pytorch profiler documentation,” 2024, accessed: 2024-12-09. [Online]. Available: <https://pytorch.org/docs/stable/profiler.html>
- [50] A. Radford, J. Wu, R. Child, D. Luan, D. Amodei, I. Sutskever *et al.*, “Language models are unsupervised multitask learners,” *OpenAI blog*, vol. 1, no. 8, p. 9, 2019.
- [51] M. Rakka, J. Li, G. Dai, A. Eltawil, M. E. Fouda, and F. Kurdahi, “Softmap: Software-hardware co-design for integer-only softmax on associative processors,” *arXiv preprint arXiv:2411.17847*, 2024.
- [52] V. J. Reddi, C. Cheng, D. Kanter, P. Mattson, G. Schmuelling, C.-J. Wu, B. Anderson, M. Breughe, M. Charlebois, W. Chou *et al.*, “Mlperf inference benchmark,” in *2020 ACM/IEEE 47th Annual International Symposium on Computer Architecture (ISCA)*. IEEE, 2020, pp. 446–459.
- [53] S. Ren, K. He, R. Girshick, and J. Sun, “Faster r-cnn: Towards real-time object detection with region proposal networks,” *Advances in neural information processing systems*, vol. 28, 2015.
- [54] M. Sandler, A. Howard, M. Zhu, A. Zhmoginov, and L.-C. Chen, “Mobilenetv2: Inverted residuals and linear bottlenecks,” in *Proceedings of the IEEE conference on computer vision and pattern recognition (CVPR)*, 2018, pp. 4510–4520.
- [55] K. Simonyan and A. Zisserman, “Very deep convolutional networks for large-scale image recognition,” *arXiv preprint arXiv:1409.1556*, 2014.
- [56] J. R. Stevens, R. Venkatesan, S. Dai, B. Khailany, and A. Raghunathan, “Softmax: Hardware/software co-design of an efficient softmax for
- [64] E. Xie, W. Wang, Z. Yu, A. Anandkumar, J. M. Alvarez, and P. Luo, “Segformer: Simple and efficient design for semantic segmentation with transformers,” *Advances in Neural Information Processing Systems*, vol. 34, pp. 12 077–12 090, 2021.
- transformers,” in *2021 58th ACM/IEEE Design Automation Conference (DAC)*. IEEE, 2021, pp. 469–474.
- [57] A. Symons, L. Mei, S. Coleman, P. Houshmand, S. Karl, and M. Verhelst, “Stream: A modeling framework for fine-grained layer fusion on multi-core dnn accelerators,” in *2023 IEEE International Symposium on Performance Analysis of Systems and Software (ISPASS)*. IEEE, 2023, pp. 355–357.
- [58] H. Touvron, L. Martin, K. Stone, P. Albert, A. Almahairi, Y. Babaei, N. Bashlykov, S. Batra, P. Bhargava, S. Bhosale *et al.*, “Llama 2: Open foundation and fine-tuned chat models,” *arXiv preprint arXiv:2307.09288*, 2023.
- [59] A. Vaswani, N. Shazeer, N. Parmar, J. Uszkoreit, L. Jones, A. N. Gomez, Ł. Kaiser, and I. Polosukhin, “Attention is all you need,” *Advances in neural information processing systems*, vol. 30, 2017.
- [60] H. Wang, Z. Zhang, and S. Han, “Spatten: Efficient sparse attention architecture with cascade token and head pruning,” in *2021 IEEE International Symposium on High-Performance Computer Architecture (HPCA)*. IEEE, 2021, pp. 97–110.
- [61] T. Wolf, “Huggingface’s transformers: State-of-the-art natural language processing,” *arXiv preprint arXiv:1910.03771*, 2019.
- [62] T. Wolf, L. Debut, V. Sanh, J. Chaumond, C. Delangue, A. Moi, P. Cistac, T. Rault, R. Louf, M. Funtowicz *et al.*, “Transformers: State-of-the-art natural language processing,” in *Proceedings of the 2020 conference on empirical methods in natural language processing: system demonstrations*, 2020, pp. 38–45.
- [63] G. Xiao, J. Lin, M. Seznec, H. Wu, J. Demouth, and S. Han, “Smoothquant: Accurate and efficient post-training quantization for large language models,” in *International Conference on Machine Learning*. PMLR, 2023, pp. 38 087–38 099.
- [65] C. Xu, X. Hou, J. Liu, C. Li, T. Huang, X. Zhu, M. Niu, L. Sun, P. Tang, T. Xu *et al.*, “Mmbench: Benchmarking end-to-end multi-modal dnn and understanding their hardware-software implications,” in *2023 IEEE International Symposium on Workload Characterization (IISWC)*. IEEE, 2023, pp. 154–166.
- [66] X. Yang, M. Gao, Q. Liu, J. Setter, J. Pu, A. Nayak, S. Bell, K. Cao, H. Ha, P. Raina *et al.*, “Interstellar: Using halide’s scheduling language to analyze dnn accelerators,” in *Proceedings of the Twenty-Fifth International Conference on Architectural Support for Programming Languages and Operating Systems*, 2020, pp. 369–383.
- [67] B. Zhang and R. Sennrich, “Root mean square layer normalization,” *Advances in Neural Information Processing Systems*, vol. 32, 2019.
- [68] J. Zhu, Y. Xia, L. Wu, D. He, T. Qin, W. Zhou, H. Li, and T.-Y. Liu, “Incorporating bert into neural machine translation,” *arXiv preprint arXiv:2002.06823*, 2020.